

Effect of random-telegraph laser phase on two-photon absorption

G. N. Sinclair,¹ X. Bao,² D. S. Elliott,³ and M. W. Hamilton⁴

¹*Defence Research Agency, St. Andrews Road, Malvern, WR14 3PS, United Kingdom*

²*Physics Department, University of New Brunswick, Fredericton, Canada E3B 5A3*

³*School of Electrical Engineering, Purdue University, West Lafayette, Indiana 47907*

⁴*Department of Physics and Mathematical Physics, University of Adelaide, South Australia 5005, Australia*

(Received 29 November 1994)

Measurements of two-photon absorption spectra have been made for the case where the exciting laser has a random-telegraph phase. The resulting spectral shapes are compared to theoretical predictions and to previous data taken with a phase-diffusing laser field [Elliott *et al.*, Phys. Rev. A **32**, 887 (1985)]. A striking dependence of the absorption spectrum on the second-order coherence of the field was observed. Using the theory for the propagation of second-order spatial coherence, we draw an analogy between diffraction and two-photon absorption which we use to interpret the two-photon absorption spectra.

PACS number(s): 42.50.Hz, 32.80.Wr, 42.50.Ne

I. INTRODUCTION

Nonlinear optical processes can show some interesting and sometimes counterintuitive effects because of their dependence on the second and higher orders of electromagnetic-field coherence, such as $G^{(4)}(t_1, t_2; t_3, t_4) = \langle E^*(t_1)E^*(t_2)E(t_3)E(t_4) \rangle$ [1]. In this paper we describe an experiment that demonstrates this dependence using two-photon absorption (TPA), which is a simple example of a nonlinear optical process as well as a useful spectroscopic tool. We spectrally broadened a laser artificially to create a field with random-telegraph (RT) phase noise and then measured absorption spectra for TPA from this field. There has been a considerable amount of interest in the effect of noise on nonlinear processes because the noise represents a relaxation that does not always manifest itself as a simple change in the time constant of an exponential decay. This is especially true of colored noise in the strong-field regime, where the energy-level population densities become coupled to the polarization. A number of experiments that test these ideas have been performed; these include the formation and destruction of atomic coherence in the Hanle effect with a strong noisy laser [2], examination of atomic population fluctuations induced by laser noise [3], and measurements of gain of a probe-laser beam interacting with strongly driven two-level atoms where both the saturating and probe lasers had a fluctuating phase and frequency [4]. The last experiment had the added interest of a time delay between the otherwise identical noise processes on each beam, thus introducing a non-Markovian character to the situation. In such experiments where saturation is studied, all orders of the field coherence are relevant.

The experiment that we describe here is a little different from those mentioned above, in that the nonlinear effect depends on just one of the higher-order coherences. This greatly simplifies the theory and facilitates a close comparison with the experimental results. A

simplifying feature of multiphoton absorption arises when the absorbed photons come from field modes that have identical fluctuations. In this case the appropriate higher-order coherence function for the calculation of the absorption spectrum can be obtained by noting that the higher-order function has exactly the same form as the lowest-order one, $\langle E^*(\tau)E(0) \rangle$, except that the phase or frequency fluctuation is amplified by a factor equal to the order of the process [5]. This prediction was confirmed in a microwave second-harmonic-generation experiment [6], where RT and Gaussian phase noise were separately applied to the exciting microwave field. Second-harmonic generation and TPA are similar processes in this context in that both depend on the same fourth-order field correlation function. The difference between them is whether the symmetry properties of the medium allow the polarization thus created to act as a source of radiation for that frequency. In our experiment with TPA in an atomic vapor this second-harmonic emission would violate conservation of angular momentum, at least insofar as the electric dipole approximation is valid. A more important difference between the second-harmonic-generation experiment and ours is that they were performed in quite different regimes of atomic or material relaxation rates, relative to the bandwidth of the exciting field. Another distinction rests with our ability to effect a decorrelation between the two field modes from which the atoms absorb. This was done in the same way as in Ref. [7], where an earlier TPA experiment with a phase-diffusing laser field was reported. Similar experiments have recently been completed that look at the effect on the TPA of amplitude noise, with and without accompanying phase fluctuations [8]. In the case of amplitude noise the interest lies not only in the resulting spectral shape, but in the total probability of absorption, which can be considerably enhanced over that for the noise-free or monochromatic case.

If the spectral broadening is the result of a frequency chirp, as occurs in many pulsed lasers, the two-photon

absorption spectrum can be shifted as well as broadened and otherwise changed in shape. Such considerations have been aired lately because of the importance of TPA as a tool in Lamb-shift measurements [9]. The concept of spectral focusing in two-photon absorption was introduced recently [10] where the temporal variation of phase in a mode-locked laser pulse (i.e., a chirp) was likened to the variation of phase across a slit in Fresnel diffraction. An analogy between diffraction and TPA was used to predict the spectral concentration of energy, initially in a fairly broad laser spectrum, to a rather narrower range around the two-photon resonance energy. In this picture the basic idea is that the observed TPA spectrum is a result of the interference of many different paths to the final state, each path consisting of a different combination of photon energies that add up to the transition energy. Actually, such a view was explored many years ago in an experiment by Bjorkholm and Liao [11], who investigated the two-photon absorption probability for the sodium $3S$ to $4D$ transition with two independently tunable dye lasers. In that experiment the phase of the paths was affected by intermediate $3P_{1/2}$ and $3P_{3/2}$ levels. For certain combinations of laser frequencies the influence of these states resulted in constructive interference, and for others, destructive interference. This interference of different paths is easier to visualize for diffraction, where the propagation is spatial, than for absorption of light, where the propagation can be thought of as occurring in an energy dimension. In this paper we will use an extension of these ideas involving expressions for the propagation of coherence that are analogous to the Fresnel-Kirchoff integral to interpret our results.

In the next section we will summarize the theoretical calculation of the TPA spectrum for a laser with RT phase noise. Then in Sec. III we will summarize the random modulation techniques and describe the two-photon absorption setup. The results of the experiment will be presented and discussed in Sec. IV, and this will be followed by a discussion of the results in light of the analogy with diffraction.

II. THEORY

The theory of TPA in fluctuating laser fields has been very well described in the literature [1], but it is helpful to extract here the main results that pertain to RT phase fluctuations. A laser with RT phase fluctuations is characterized by an electric field of the form

$$E(t) = E_0 e^{-i[\omega_0 t + \phi(t)]}, \quad (1)$$

where ω_0 is the mean angular frequency, E_0 is the constant field amplitude, and $\phi(t)$ is the fluctuating phase. The phase jumps between two fixed values at random times, such that the probability of n transitions in a time T_0 is given by the Poisson distribution

$$P(n) = \frac{(\bar{n})^n e^{-\bar{n}}}{n!}. \quad (2)$$

The mean number of jumps in time T_0 is \bar{n} and we define the dwell time (i.e., the mean time between transitions) as

$$T = T_0 / \bar{n}.$$

The power spectral density of the laser (which we loosely refer to as the power spectrum) is calculated according to the Wiener-Khintchine theorem from the first-order coherence function $\langle E^*(\tau)E(0) \rangle$. In the case of RT phase noise this is given by

$$\langle E^*(\tau)E(0) \rangle = E_0^2 \left[\cos^2 \left[\frac{\Phi}{2} \right] + \sin^2 \left[\frac{\Phi}{2} \right] e^{-(2/T)|\tau|} \right] e^{i\omega_0 \tau}, \quad (3)$$

where Φ is the total size of the phase jump. The correlation time of the noise is seen to be $2/T$. The power spectrum is then

$$S(\omega) = 2\pi [E_0]^2 \left[\delta(\omega - \omega_0) \cos^2 \left[\frac{\Phi}{2} \right] + \frac{2}{\pi T} \frac{1}{(\omega - \omega_0)^2 + \left[\frac{2}{T} \right]^2} \sin^2 \left[\frac{\Phi}{2} \right] \right]. \quad (4)$$

In communication engineering terms this power spectrum is comprised of two parts: a δ -function carrier and Lorentzian-shaped noise sidebands. The relative power in each part is determined by the strength of the noise; i.e., the size of the phase jump Φ . The correlation time of the noise, $2/T$, determines the width of the continuum part of the spectrum. This contrasts with the case of a laser broadened by Gaussian phase noise (i.e., an Ornstein-Uhlenbeck process), where the noise amplitude and correlation time together determine the width and spectral shape of the laser field [12]. Note that the spectrum (4) reduces to a Lorentzian if $\Phi = \pi$.

Nonlinear optical processes depend on the higher-order coherences of the laser field; i.e., we must be able to specify field correlation functions of an order higher than $\langle E^*(\tau)E(0) \rangle$. Two-photon absorption in the low-field regime depends on the next-highest-order nonzero correlation function $\mathcal{G}^{(4)}(t_1, t_2; t_3, t_4)$. It is important to consider this dependence in the context of the usual Doppler-free setup for two-photon spectroscopy [13], which we used for these measurements; see Fig. 1. The Doppler shift due to the atomic motion in the laser propagation direction(s) is cancelled because two counterpropagating laser beams are used; one photon is absorbed from each beam, their Doppler shifts being equal but opposite in sign. The forward and backwards propagating beams in our experiment were produced by placing a retroreflecting mirror in the laser beam after it had passed once through the cell. This allows for the possibility that the fluctuations in the retroreflected beam, at the atoms, may be partially decorrelated from those of the incoming beam. This degree of decorrelation is specified by τ_r , the time taken by the light to travel from the atoms to

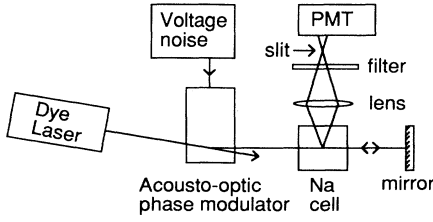


FIG. 1. Simplified schematic of the two-photon absorption experiment with a randomly modulated laser. The photomultiplier that detects fluorescence is the PMT. Beam splitters that pick off the beam at various points for laser spectral diagnostics are not shown.

the mirror and back again.

We first consider the case where the mirror is close enough to the atoms that τ_r is negligible. Then the two-photon absorption rate as a function of laser center-frequency, i.e., the absorption spectrum, is

$$W_2(\omega_0) = |g(\omega_0)|^2 \int_{-\infty}^{\infty} \mathcal{G}^{(4)}(\tau, \tau; 0, 0) e^{-i\omega_f \tau - \kappa|\tau|/2} d\tau, \quad (5)$$

where $g(\omega_0)$ is a factor containing the dipole matrix elements connecting the lower (or upper) level with the intermediate level, $\hbar\omega_f$ is the final-state-initial-state energy difference, and κ is the natural full width at half maximum (FWHM) of the transition [1]. This equation is valid if $2\omega_0 \approx \omega_f$ and the spectral width of the laser $\Delta\omega \ll \omega_f$, conditions that are easily fulfilled in the optical regime where $\Delta\omega \sim 10^7 \text{ s}^{-1}$ and $\omega_0 \sim 10^{15} \text{ s}^{-1}$.

If there are no real energy levels close to the intermediate levels, then $g(\omega_0)$ is essentially a constant. For the sodium $3S$ to $5S$ two-photon transition that we use, the $3P$ level is sufficiently close to the intermediate levels to enhance the rate of absorption without making $g(\omega_0)$ vary significantly over the ranges of laser scan frequencies ($\sim 100 \text{ MHz}$) or Fourier components ($\sim 500 \text{ MHz}$) of interest. In Eq. (5) the decay rate κ is that of the polarization [14]. Since in fact we have some collisional

broadening as well as spontaneous decay, we take κ to be the residual width (without laser noise) of the TPA spectrum. If the atomic response is Lorentzian, which is very nearly the case if the only sources of broadening are natural broadening and collisions, and the collisional rate is similar to the spontaneous emission rate, then the resulting spectrum is composed of two superposed Lorentzians, one with full width κ and the other with full width $\kappa + 4T^{-1}$,

$$W_2(\omega_0) \propto E_0^4 \left\{ \frac{\frac{\kappa}{2}}{(\omega_f - 2\omega_0)^2 + \left(\frac{\kappa}{2}\right)^2} \cos^2(\Phi) + \frac{\frac{\kappa}{2} + \frac{2}{T}}{(\omega_f - 2\omega_0)^2 + \left(\frac{\kappa}{2} + \frac{2}{T}\right)^2} \sin^2(\Phi) \right\}. \quad (6)$$

Comparing (6) with (4) we see that if $\Phi = \pi$ and $\kappa \rightarrow 0$, $S(\omega)$ is a pure Lorentzian but $W_2(\omega_0)$ tends to a δ function. Even with the residual width of the transition taken into account the result is that the width of $W_2(\omega_0)$ is independent of that of $S(\omega)$. The relative power within the two components is still determined by the size of the phase jump. Extending the above discussion to the case where the round trip time τ_r is important, we find through a simple extension of the theory [1,7] that

$$W_2(\omega_0) = |g(\omega_0)|^2 \int_{-\infty}^{\infty} \mathcal{G}^{(4)}(\tau, \tau + \tau_r; 0, \tau_r) \times e^{-i\omega_f \tau - \kappa|\tau|/2} d\tau. \quad (7)$$

In calculating the correlation function, we need to identify the two cases $\tau > \tau_r$ and $\tau < \tau_r$. For the random-telegraph phase we have, if $\tau > \tau_r$,

$$\mathcal{G}^{(4)}(\tau, \tau + \tau_r; 0, \tau_r) = E_0^4 e^{2i\omega_0 \tau} \{ \cos^4(\theta) + e^{-4\tau_r/T} \sin^4(\theta) - \sin^2(\theta) \cos^2(\theta) [2e^{-2\tau_r/T} - e^{-2\tau/T} (e^{\tau_r/T} + e^{-\tau_r/T})^2] \}, \quad (8a)$$

and if $\tau < \tau_r$,

$$\mathcal{G}^{(4)}(\tau, \tau + \tau_r; 0, \tau_r) = E_0^4 e^{2i\omega_0 \tau} \{ \cos^4(\theta) + e^{-4\tau/T} \sin^4(\theta) - \sin^2(\theta) \cos^2(\theta) [2e^{2\tau_r/T} - (2e^{-2\tau/T} + e^{-2(\tau_r - \tau)/T} + e^{-2(\tau_r + \tau)/T})] \}, \quad (8b)$$

where $\theta = \Phi/2$. Letting $\Delta = 2\omega_0 - \omega_f$, $\gamma_1 = \kappa/2$, $\gamma_2 = \kappa/2 + 4/T$, $\gamma_3 = \kappa/2 + 2/T$, $\gamma_4 = \kappa/2 - 2/T$, $\rho = \exp[-2\tau_r/T]$, $\mathcal{L}(\Delta, \gamma) = \gamma/(\gamma^2 + \Delta^2)$, and $P(\Delta, \gamma) = \cos(\Delta\tau_r) - (\Delta/\gamma) \sin(\Delta\tau_r)$, we get the TPA spectrum

$$W_2(\omega_0) \propto E_0^4 \{ \mathcal{L}(\Delta, \gamma_1) \{ \cos^4(\theta) - [\frac{1}{2}\rho \sin^2(\Phi) + \rho^2 \sin^4(\theta) e^{-\gamma_1 \tau_r} P(\Delta, \gamma_1)] \} + \mathcal{L}(\Delta, \gamma_2) \{ \sin^4(\theta) [1 - e^{-\gamma_2 \tau_r} P(\Delta, \gamma_2)] \} + \mathcal{L}(\Delta, \gamma_3) \{ \frac{1}{4} \sin^2(\Phi) [2 + \rho + \rho^{-1} e^{-\gamma_3 \tau_r} P(\Delta, \gamma_3)] \} + \mathcal{L}(\Delta, \gamma_4) \{ \frac{1}{4} \sin^2(\Phi) \rho [1 - e^{-\gamma_4 \tau_r} P(\Delta, \gamma_4)] \} \}. \quad (9)$$

The delay τ_r has two main effects on the two-photon absorption spectrum. First, it introduces two new components, which, in the limit of long delay time ($\tau_r \gg \gamma_2^{-1}$, γ_4^{-1}), tend towards Lorentzian-shaped peaks of widths γ_2 and γ_4 . The amplitude of the latter, however, vanishes in this limit of long delay time due to the factor ρ included there. This term is rather unusual in that its width is the *difference* between the laser linewidth and the atomic linewidth. Thus as the laser width and atomic width approach one another, the width of this peak tends towards zero (i.e., a δ function), but at the same time the amplitude of this peak, $1 - e^{-\gamma_4 \tau_r} P(\Delta, \gamma_4)$, approaches zero. In the event of γ_4 being negative, the factor ρ again ensures that the contribution of the $\mathcal{L}(\Delta, \gamma_4)$ term remains small. Thus, overall, this term is not expected to contribute much to the line shape, and was not observed in our measurements at all since we used $\Phi = \pi$.

The second influence of a nonzero delay time τ_r is that each of the four components of the absorption line shape becomes non-Lorentzian, as expressed by the function $P(\Delta, \gamma_i)$, $i=1, \dots, 4$. This term can be significant. Note that this function is always symmetric in Δ , and that in the limit $\tau_r \rightarrow 0$, $P(\Delta, \gamma)$ reduces to unity for all Δ, γ . In this limit, the amplitudes of the Lorentzian peaks $L(\Delta, \gamma_2)$ and $L(\Delta, \gamma_4)$ reduce to zero, and the absorption line shape of Eq. (9) is equivalent to that of Eq. (6). It is only in this limit that the two-photon absorption width is independent of laser width with $\Phi = \pi$. Finally, we remark on the line shape in the limit $\gamma_i \tau_r \gg 1$. In this case three Lorentzian peaks of half-widths $\kappa/2$, $\kappa/2 + 2/T$, and $\kappa/2 + 4/T$ survive. The two counterpropagating beams are decorrelated, since the round trip delay is longer than the correlation time of the optical field. The absorption line shape is then expected to contain terms of width as large $\kappa/2 + 4/T$, since this is the result of a convolution of three Lorentzians (one of width $\kappa/2$ and two of width $2/T$) with each other. Thus for $\gamma_i \tau_r \gg 0$, the absorption linewidth varies linearly with laser linewidth. For smaller $\gamma_i \tau_r$, the relation between absorption linewidth and laser linewidth is more complex, and we have used numerical analysis for comparison with our experimental results.

By comparison, we note that with phase and frequency fluctuations that correspond to an Ornstein-Uhlenbeck process (the phase-diffusing laser) and Lorentzian-shaped laser spectrum is also possible in the limit where the correlation time of the noise is very short. The TPA spectrum that results is a Lorentzian with a width two times that of the laser, where the former is measured in terms of the laser frequency scan [7]. By forcing the field amplitude to fluctuate in such a way that the phase remains constant, the real Gaussian field [8], one can also realize a Lorentzian-shaped laser power spectrum. In this case the resulting two-photon absorption spectrum is a composite of two Lorentzians, one with the natural width of the transition, and the other with the width of the laser spectrum plus the natural width. This is similar behavior to that predicted above in Eq. (7), except that with the real Gaussian field the ratio of powers within each Lorentzian is fixed.

III. EXPERIMENT

The principle of the experiment is to observe TPA, having imposed electronic noise on the laser phase. By maintaining laser noise due to environmental perturbations at a low level, the fluctuations of our generated field can easily be characterized statistically by performing appropriate measurements on the electronic noise. There is a variety of ways of making laser fields with Lorentzian-shaped power spectra. As noted above, one such route to a Lorentzian spectrum is to have RT phase noise where the size of the phase jump $\Phi = \pi$. TPA data obtained with the field having RT phase fluctuations (with $\Phi = \pi$) can be compared to the data from the experiment in Ref. [7], where the phase-diffusing laser spectrum was also approximately Lorentzian. Since each method will give a different form of $\mathcal{G}^{(4)}(t_1, t_2; t_3, t_4)$, different two-photon absorption spectra are to be expected.

The layout of the TPA experiment is shown schematically in Fig. 1. It was the usual Doppler-free configuration with counterpropagating beams [13]. When the laser was scanned through the sodium 3S to 5S resonance, at about a 602 nm wavelength, atoms were excited to the 5S level (lifetime 80 ns). The laser power was typically about 80 mW, focused to a waist of order 100 μm diameter in the sodium cell, which was operated at 157°C. The intensity thus produced was well below that required to saturate the transition, and thus the theoretical approach based on perturbation theory [1] is appropriate. One decay channel from the 5S level involved emission from the 4P level at a 330-nm wavelength. A photomultiplier detected the 330-nm wavelength radiation, and the strength of this fluorescence was used as a measure of the TPA rate. The slit and the filter shown in front of the photomultiplier in Fig. 1 were used to exclude stray laser light. The interaction region in the cell was imaged onto the slit so that stray laser radiation scattered from the cell windows was not incident on the filter. This was a piece of colored glass intended for blocking visible light and transmitting ultraviolet light, but was insufficient on its own to block all stray laser light. The cell itself was a fused silica cube, 1 cm on a side, containing a minimal quantity of sodium so that coating and browning of the windows by the metal was not a problem. At the distillation of sodium into the cell a very small quantity of sodium metal was visible in the cell, which disappeared after the first heating to the operating temperature. Thus on subsequent reheating of the cell we can place an upper limit, based on published vapor pressure data, of about 10^{13} cm^{-3} for the number density of sodium atoms. Residual gas from the filling was present and broadened the transition from a natural width of 1 MHz to about 7 MHz [i.e., half width at half maximum (HWHM) measured in terms of the laser frequency scan, rather than the total energy absorbed].

The absorption spectrum consisted of two well-resolved hyperfine components, $F=1$ to $F=1$ and $F=2$ to $F=2$, which were 808 MHz apart [13] and each of width ~ 10 MHz with no laser noise present. These frequencies are also in terms of the laser frequency scan. In

our comparisons of the observed and theoretical spectra we concentrated on the $F=2$ to $F=2$ peak, which was the stronger one. The Doppler broadened background, which was expected because we used linearly polarized light, was not observable because of the detection noise. Most of the detection noise was due to the low number of atoms in the interaction region.

The details of the techniques for random modulation of the laser are the subject of a separate report [15], but for completeness a brief summary of the pertinent points is given here. The arrival of photons at a photomultiplier tube (PMT) was exploited to generate the phase jumps. Note that this was not the same PMT that viewed fluorescence from the sodium, but a second one that detected photons from an incandescent bulb. The photocurrent pulse statistics were governed by Eq. (2) when the detection efficiency was low, even for light sources that had non-Poissonian emission statistics. Dead-time effects in the PMT can, however, cause non-Poissonian counting statistics if the counting rate is too high, which imposed a practical lower limit on the dwell time of about 40 ns. The photocurrent pulses from the PMT anode were amplified and directed to the clock input of a divide-by-two counter whose output was the raw RT signal. This voltage was analyzed in order to confirm that Eq. (2) holds. For dwell times greater than 40 ns the distribution is acceptably close to Poissonian. The criterion used for acceptability was that the variance be within 10% of the mean. The RT voltage probability distribution was also checked to be sure that the high and low states were equally likely.

The next stage was to map the voltage fluctuations into phase fluctuations by using an optical modulation technique. Two techniques were developed; the first made use of an acousto-optic modulator (AOM) to produce phase jumps of π radians. This is illustrated in Fig. 2(a). The AOM was a Crystal Technology model 3200 that had a nominal rf drive frequency of 200 MHz. A biphasic modulator switched the phase of the rf drive signal by π radians at times determined by the transitions of the RT voltage described above. The first-order diffracted beam from the AOM has this phase shift of π imposed on it. In Fig. 2(b) we show an example of the laser power spectrum obtained with this type of modulation. As expected from Eq. (4) the carrier part of the spectrum is completely suppressed, leaving only the Lorentzian-shaped noise

sidebands. The solid curve is a Lorentzian fitted to the measured spectrum. Note that this spectrum is plotted with a linear vertical scale. The laser power spectra were measured by observing on an rf spectrum analyzer the beat signal between portions of the modulated and unmodulated beams. As part of the random modulation process a frequency shift was imposed on the modulated first-order beam so that the beat signal was centered on the AOM drive signal frequency of 200 MHz. The power spectrum of this beat signal was a downshifted version of the optical power spectrum. A limitation of this modulation technique was that the phase jump had a finite rise time of some 20 ns, which resulted in a small directional shift of the beam during the transition so that the spectrum of the beam was not completely uniform across the beam. The reason for this limitation and prospects for overcoming it are discussed in the next section. Figure 2(b) was obtained near the center of the modulated beam and shows a slight asymmetry because of this rise-time effect; spectra obtained closer to the edges of the beam show rather more asymmetry. Because of this we preferred to use an electro-optic modulator (EOM) for smaller phase jumps, although AOM's can be used for creating arbitrary phase shifts [16].

The second technique used a traveling-wave electro-optic phase modulator to impose phase jumps of up to 2 rad. With this method, laser power spectra agreeing with Eq. (4) could be obtained. We will not discuss this method further, except to mention the fact that although the phase-transition time was shorter (~ 4 ns), rf heating effects that caused spurious amplitude modulation limited the size of the phase jump to about 2 rad. We did take TPA data with the EOM but the data are inconclusive because κ and $1/T$ are of similar size. In this regime of $\Phi < \pi$ the data are of limited interest, unless the shape of the spectrum can be unambiguously determined. Although the sum of two Lorentzians can be fitted to the resulting TPA spectra, as indicated by Eq. (6), a single Lorentzian function can be fitted equally well for the value of κ and the range of $1/T$ that we had available. It is easily verified that the sum of two Lorentzians with widths of similar size is very similar in shape to that of a single Lorentzian.

With the above apparatus (AOM) we measured TPA spectra for a variety of dwell times, using π radian phase jumps, by scanning the laser through the TPA resonance.

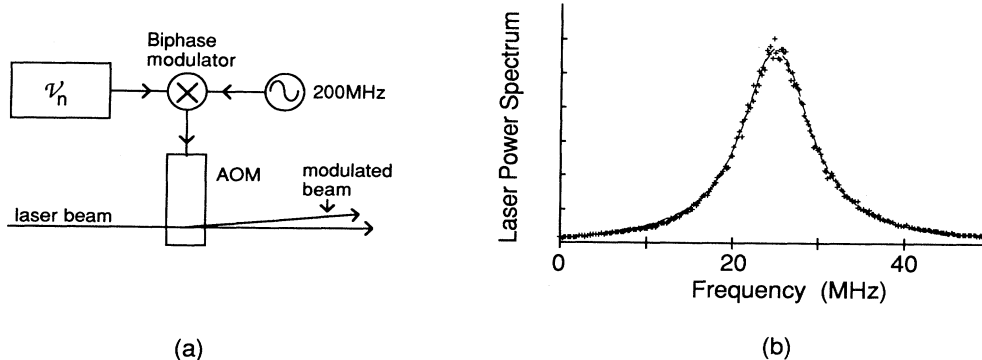


FIG. 2. (a) Schematic of the technique for imposing π radian random-telegraph phase noise. The RT voltage source is denoted by the box labeled \mathcal{V}_n . A more detailed picture can be found in Ref. [16]. (b) An example of a laser spectrum obtained with the setup in (a). The crosses are data and the solid line is a Lorentzian fit. The dwell time T is 67 ns, giving the FWHM of 9.5 MHz. Note that the vertical scale is linear.

Dye laser scans over these relatively short frequency ranges (~ 100 MHz) are usually fairly nonlinear, and our experiment was no exception. To overcome this we separately calibrated each scan with a spherical mirror Fabry-Pérot interferometer, which was built so that the non-TEM₀₀ modes could also be used as frequency markers. This kept the overall length of the interferometer manageable. A number of scans (typically ten) with the same values of Φ and T could then be added, to improve the signal-to-noise ratio, after having their frequency scans separately calibrated.

IV. RESULTS AND DISCUSSION

For the experiments with $\Phi = \pi$ and $\tau_r = 0$, we expect the TPA spectra to be just the same as if there were no laser noise at all; i.e., the widths of the spectra should be independent of the strength of the noise. One set of TPA data is shown in Fig. 3 with a Lorentzian fitted to it. This spectrum is the average of ten individual spectra that have had their frequency axes separately calibrated to remove scan nonlinearities before being added. In Fig. 4(a) we show the widths extracted from such fits plotted against the width of the laser power spectrum. The widths of the laser spectra were similarly obtained by fitting Lorentzians to the data. Also shown for comparison are data from Ref. [7], where the exciting laser had a phase that was an Ornstein-Uhlenbeck process (phase diffusion). The laser spectra resulting from this and from the RT phase are very similar, both being approximately Lorentzian but falling off somewhat more rapidly in the wings than would a Lorentzian. The difference in the trend of each set of data with increasing laser width clearly reflects the fact that TPA depends on the second-order coherence of the field. For RT noise in the limit of small τ_r , there is agreement with the prediction that the TPA width will be independent of the laser spectral width [17]. This can be understood by noting that the absorption probability amplitude depends on $E(t)^2$, and in the random-telegraph case the phase jump of 2π that we then find in $E(t)^2$ leaves $\mathcal{G}^{(4)}(\tau, \tau; 0, 0)$ essentially unchanged from the noise-free case. This is not the case for the phase-diffusing field, where the phase difference be-

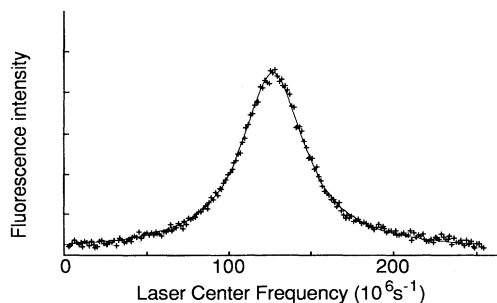


FIG. 3. Example of TPA spectrum obtained with the RT phase on the laser ($\Phi = \pi$). The value of T is 237 ns (laser FWHM = 2.7 MHz) and $\tau_r = 2.6$ ns. The data are indicated by crosses.

tween the two photons is not so restricted. A more complete intuitive picture based on this observation, which takes into account the possibility $\Phi \neq \pi$, is not so easy, however, and we take up this point in the next section.

Shown in Fig. 4(b) are data where τ_r was increased from 2.6 to 10.8 and 22.8 ns. The data for $\tau_r = 2.6$ ns are the same as those shown in Fig. 4(a). It is clear that for larger values of τ_r , the data agree qualitatively with the general prediction of Eq. (9) that the TPA spectral width should increase with increasing laser spectral width. Quantitatively, the agreement is good for $\tau_r = 10.8$ ns but not for $\tau_r = 22.8$ ns. In this figure we have extracted the widths of the TPA spectra by fitting simple Lorentzians. When the various parameter values pertinent to the experiment are inserted into Eq. (9), the resulting spectrum has a shape that is little different from a Lorentzian, and the signal-to-noise ratio in the wings of the observed

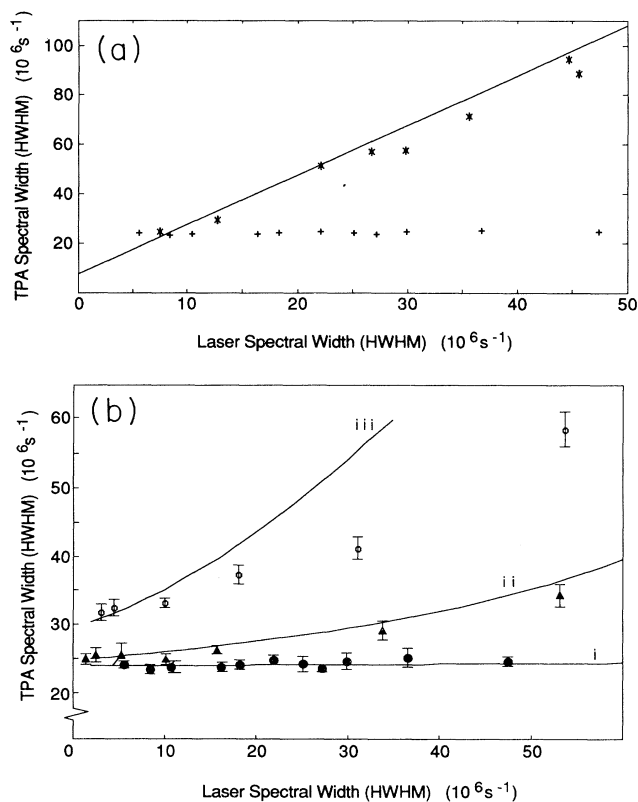


FIG. 4. (a) Summary of TPA spectral data for case of negligible τ_r (2.6 ns); +, widths of Lorentzians fitted for data for the RT phase ($\Phi = \pi$); *, widths of spectra for the phase-diffusing laser case (from Ref. [7]). The solid line is from Ref. [7] and indicates the linear dependence of the TPA spectral width on the phase-diffusing laser width. In both cases the laser has a Lorentzian-shaped power spectrum. (b) TPA spectral widths (from fitted Lorentzians) for the RT phase ($\Phi = \pi$) for varying τ_r , ●, $\tau_r = 2.6$ ns; ▲, $\tau_r = 10.8$ ns; ○, $\tau_r = 22.8$ ns. The solid lines are the spectral widths as determined by analysis of Eq. (9) and are numbered (i) $\tau_r = 2.6$ ns, (ii) $\tau_r = 10.8$ ns, (iii) $\tau_r = 22.8$ ns. The data for $\tau_r = 2.6$ ns are the same as those shown in (a).

spectrum is not good enough to distinguish the differences between a single Lorentzian and the more correct form of Eq. (9). The theoretical widths plotted in Fig. 4(b) are from Eq. (9), however. The discrepancy for $\tau_r = 22.8$ ns is unresolved. There are a number of possible reasons for the discrepancy that are worth future investigation. The phase jumps have a finite duration, but the theoretical treatment outlined in this paper implicitly assumes that the transitions are instantaneous. Extension of the theory to cover this situation seems to be warranted. Also, improvement of the experimental technique to shorten the transition time while still allowing π radian phase jumps would be useful. There is a number of possible ways to do this, though it is not clear which will be best in the end. The main limitation of an AOM is the speed of sound in the AOM crystal, and more than an order of magnitude increase would be needed to significantly improve our rise time. A smaller improvement may also be made by increasing the rf drive frequency, which allows the laser waist to be made smaller without sacrificing the diffraction efficiency. It seems that the most significant technical improvements could come from advances in EOM technology. Guided wave devices can easily give π radian phase shifts for just a few volts of input. These have been, until recently, available commercially only for the communications wavelength band 1.3 to 1.5 μm but are now available for use at 800 nm. [Waveguide modulators for the visible, based on potassium titanyl phosphate (KTP), have been developed but are not commercially available.]

V. THE TPA-DIFFRACTION ANALOGY

In a recent report, Broers, Noordam, and van Linden van den Heuvell [10] explored an analogy between the diffraction of light by a narrow slit and two-photon absorption of a coherent short-duration pulse. Based on this analogy, they were able to construct a "spectral Fresnel zone plate," allowing them to concentrate the spectral energy at the two-photon level into a bandwidth narrower than the bandwidth of the laser. In this section, we consider the case of two-photon excitation by partially coherent light and show that a similar analogy with diffraction processes can be established. Such an analogy allows one to gain some intuitive insight into the TPA process when partially coherent light is involved.

For frequency chirped pulses, Broers *et al.* observe that, when the spectrum of the field is symmetric about a frequency ω_0 , the two-photon process is in principle the same as a linear process driven by an effective field of the form

$$E^{(2)}(2\omega_0) = \int_{-\infty}^{\infty} d\omega' |E(\omega')|^2 e^{i2\phi(\omega')}. \quad (10)$$

Here $E(\omega)$ is the Fourier transform of the field $E(t)$ and $\phi(\omega)$ is the frequency-dependent phase. This is analogous to the expression for the intensity of light (on axis) after it passes through a single slit,

$$|E(x=0)|^2 = \int_{-\infty}^{\infty} dx' |E(x')|^2 e^{i\phi(x')}, \quad (11)$$

where $\phi(x')$ is the phase lag or lead caused by the ray traveling from source to detector (at $x=0$ in the plane A) via a point x' on the plane A' that holds the slit, as shown in Fig. 5. As presented, this analogy is not applicable to the measurements reported here because it can only deal with coherent broadening of the laser spectrum, as in a chirped pulse. At least if the laser is ideal, the pulse with a frequency chirp is coherent in the sense that there is a well-defined phase relationship between different frequency components of the pulse.

In order to describe the situation where the variation of the field is stochastic we refer to Wolf [18], who showed that spatial coherence functions obey the same kinds of propagation laws through space (albeit somewhat more complicated) as do waves. The propagation of the spatial coherence

$$\mathcal{G}^{(4)}(x_1, x_2, x_3, x_4) = \langle E^*(x_1)E^*(x_2)E(x_3)E(x_4) \rangle$$

can be written in integral form in a straightforward way. This spatial coherence is analogous to the temporal coherence function that appears in the TPA range [Eq. (5)], if we let $x_1 = x_2$ and $x_3 = x_4$. We will limit our analogy to the case $\tau_r = 0$ in order to simplify the algebra and to make the problem easier to visualize. We define a complex field $P(x, t) = E^2(x, t)$, since $\mathcal{G}^{(4)}(t_1, t_1; t_3, t_3)$ is just the first-order coherence of a different complex field, namely $P(t)$. Then the expression for the TPA spectrum becomes

$$W_2(\omega_0) = \int_{-\infty}^{\infty} \langle P^*(\tau)P(0) \rangle e^{-i\omega_f\tau - \kappa|\tau|/2} dt. \quad (12)$$

Since the laser bandwidth is much narrower than the center optical frequency ω_0 , we can write

$$E(t) = \tilde{E}(t)e^{-i\omega_0 t}, \quad (13)$$

where $\tilde{E}(t)$ is a complex amplitude consisting of constant and stochastic components. Equation (12) then becomes

$$W_2(\omega_0) = \int_{-\infty}^{\infty} \langle \tilde{P}(\tau)\tilde{P}(0) \rangle e^{-i\Delta\tau - \kappa|\tau|/2} dt, \quad (14)$$

where $\Delta = \omega_f - 2\omega_0$ is the detuning of the laser frequency from resonance with the two-photon transition and $\tilde{P}(t) = \tilde{E}^2(t)$. Thus the two-photon absorption spectrum is expressed as the Fourier transform of the product of

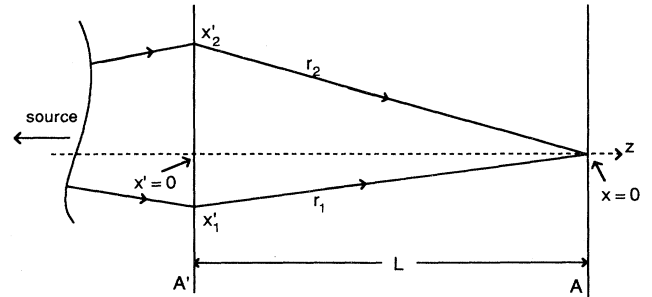


FIG. 5. Geometry of situation considered in the diffraction-TPA analogy. The detector plane is A and the aperture plane is A' .

the first-order coherence function of $\bar{P}(t)$ and the exponential term representing the finite lifetime of the excited state.

The analogy with spatial diffraction is a result of the similar relation for the propagation of the first-order coherence of the complex electric field $\mathcal{G}^{(2)}(x'_1, x'_2)$ [18],

$$\mathcal{G}^{(2)}(x_1, x_2) = \int_{-\infty}^{\infty} dx'_1 dx'_2 \frac{\mathcal{G}^{(2)}(x'_1, x'_2)}{r_1 r_2} \times \exp \left[i\omega \left[\frac{r_1 - r_2}{c} \right] \right] \Lambda_1 \Lambda_2. \quad (15)$$

The geometry for this spatial diffraction problem is again the same as shown in Fig. 5. This expression is valid in the limit of $r_{1,2} \gg \lambda$ and when the fields are stationary. We now reinterpret $\mathcal{G}^{(2)}$ as the first-order correlation function of $\bar{P}(x')$. If we take $x_1 = x_2$, then $\mathcal{G}^{(2)}(x_1, x_1)$ is the square of the intensity at the observation screen A in Fig. 5. We denote this integral as $\bar{I}(x_1)$ (to be distinguished from ordinary intensity, which in fact it would be, to within a factor of $\frac{1}{2}\epsilon_0 c$, if $\mathcal{G}^{(2)}$ had its more usual interpretation). The obliquity factors Λ_1 and Λ_2 are the squares of the usual factors for the electric field. In the limit of L much greater than any transverse dimension of interest x_1, x'_1 or x'_2 , for instance, $r_1 - r_2$ reduces to

$$r_1 - r_2 \cong \frac{1}{2L} [(x'_1 - x'_2)(x'_1 + x'_2 - 2x_1)], \quad (16)$$

and $\Lambda_i \approx 1$. In the TPA experiment the electric field, and thus also $\bar{P}(t)$, is a stationary process, so in the analog $\mathcal{G}^{(2)}(x'_1, x'_2)$ depends only on $x'_1 - x'_2$. Thus we can transform the variables in the slit plane so that $x' = x'_1 - x'_2$ and $\bar{x}' = x'_1 + x'_2$, and we write $\mathcal{G}^{(2)}(x'_1, x'_2) = \mathcal{G}^{(2)}(x')$. This transformation allows us to write

$$\bar{I}(x_1) = \frac{1}{2} \int dx' d\bar{x}' \frac{\mathcal{G}^{(2)}(x')}{r_1 r_2} \exp \left[i \frac{\pi x'}{L\lambda} (\bar{x}' - 2x_1) \right], \quad (17)$$

where we have also used $\omega/c = 2\pi/\lambda$. Finally, we impose a restriction on the aperture width, $w \ll \sqrt{L\lambda}$. This implies that our diffracting aperture is entirely within the first Fresnel zone, so we can set r_1 and r_2 equal to L when these distances appear in the denominator. We can also set $\Lambda = \Lambda_1 \approx \Lambda_2$, and we can ignore the phase variation term $\pi x' \bar{x}' / L\lambda$ since the maximum value anywhere within the aperture is $\sim w^2 / L\lambda \ll 1$. We are then led to the following expression for the $\bar{I}(x_1)$ in the observation plane A ,

$$\bar{I}(x_1) = \frac{w}{L^2} \int dx' \mathcal{G}^{(2)}(x') e^{-ikx'}, \quad (18)$$

where $k = 2\pi x_1 / L\lambda$ represents the x component of the propagation vector of a plane wave directed toward the position x_1 in the observation screen. This equation is just a specialization of the Fresnel-Kirchoff integral in diffraction, and can be compared to Eq. (14), which gives the two-photon absorption rate. From the comparison we see that the detuning from resonance Δ is analogous to k , which is linearly related to the position in the screen A , while the position within the aperture plane x' relates to

τ . An amplitude or phase mask can be introduced at the aperture plane to produce the variations of the transmitted field, analogous to the stochastic variations of the field driving the two-photon absorption process. The correlation time of the latter is transformed to the correlation distance in the aperture plane of the former. As defined thus far, nothing related to the natural linewidth of the transition has been introduced. This can be imposed by positioning a second phase mask in the aperture plane. This phase mask induces an additional phase shift in the transmitted beam, statistically independent of the fluctuations imposed by the first mask. By using phase fluctuations, which are correlated as

$$\langle [\varphi(x_1) - \varphi(x_2)]^2 \rangle = |x_1 - x_2| l_c^{-1}, \quad (19)$$

the exponential lifetime factor can be reproduced. The natural decay lifetime of the atom is then related to the correlation length l_c of this second aperture plane diffraction mask. The aperture width w must be large compared with the correlation length of either of the diffraction masks. If we take τ , into account, the same principles hold, except that we cannot make the simplifying (from a point of view of visualization) reduction of the order of the coherence function.

In the case of RT phase noise, we place a phase grating in the aperture plane. The phase grating introduces a phase delay of either Φ_1 or Φ_2 or the transmitted light, where $\Phi_1 - \Phi_2 = 2\Phi$. (Φ is the total size of the phase jump for the temporally fluctuating fields inducing the two-photon transition.) The times of the phase steps must be random and governed by the Poisson distribution. The phase grating analogous to the $\Phi = \pi$ phase jumps has a step size of $\Phi_1 - \Phi_2 = 2\pi$. Clearly a 2π phase shift has no observable effect on the spatially diffracted pattern, and the diffraction results only from the second aperture plane mask that simulates the lifetime of the excited state. This result is similar to the two-photon absorption spectrum, in which the absorption width is determined only by the homogeneous width of the atoms, and not by the laser linewidth.

For the case analogous to $\Phi = \pi/2$ temporal phase jumps, the spatial phase grating must have $\Phi_1 - \Phi_2 = \pi$. This grating clearly has a large effect on the transmitted field, as the fields transmitted by adjacent steps of the grating are of opposite sign. Using arguments similar to those leading to Eq. (3), we can show that

$$\mathcal{G}^{(2)}(x') = E_0^2 \exp \left[-\frac{2}{\xi} |x'| \right], \quad (20)$$

where ξ is the mean distance between transitions in the grating. It is clear that such a grating will produce spreading of the forward transmitted light, the spread having two contributions, one proportional to $1/\xi$, the other proportional to l_c^{-1} . The point spread function

that it produces is Lorentzian.

Using this prescription then, we can formulate aperture phase and amplitude masks that are capable of reproducing far-field patterns analogous to the effective two-photon absorption probability. We see from this discussion that this analogy is not limited to the case of coherent fields, but includes stochastic fields as well, and it helps us to gain some intuitive insight into TPA processes, at least for the case $\tau_r=0$, where second-order coherences are involved.

ACKNOWLEDGMENTS

Helpful discussions with Dr. R. J. Ballagh are gratefully acknowledged. The experimental work was performed at the University of Stathclyde, Glasgow, Scotland, to which we are obliged, and was supported by the SERC, the Wolfson Foundation, and the Research Corporation Trust. The participation of D.S.E. was made possible by a collaborative research grant from the NATO Scientific Affairs Division.

-
- [1] B. R. Mollow, *Phys. Rev.* **175**, 1555 (1968).
 - [2] K. Arnett, S. J. Smith, R. E. Ryan, T. Bergeman, H. Metcalf, M. W. Hamilton, and J. R. Brandenburger, *Phys. Rev. A* **41**, 2580 (1990).
 - [3] M. H. Anderson, R. D. Jones, J. Cooper, S. J. Smith, D. S. Elliott, H. Ritsch, and P. Zoller, *Phys. Rev. Lett.* **64**, 1346 (1990).
 - [4] M. H. Anderson, G. Vemuri, J. Cooper, P. Zoller, and S. J. Smith, *Phys. Rev. A* **47**, 3202 (1993).
 - [5] K. Wódkiewicz and J. Eberly, *J. Opt. Soc. Am. B* **3**, 628 (1986).
 - [6] R. Boscaino and R. N. Mantegna, *Phys. Rev. A* **36**, 5482 (1987).
 - [7] D. S. Elliott, M. W. Hamilton, K. Arnett, and S. J. Smith, *Phys. Rev. A* **32**, 887 (1985).
 - [8] C. Chen, M. Rifani, J. Cha, Y-Y. Yin, and D. S. Elliott, *Phys. Rev. A* **49**, 461 (1994).
 - [9] M. S. Fee, K. Danzmann, and S. Chu, *Phys. Rev. A* **45**, 4911 (1992).
 - [10] B. Broers, L. D. Noordam, and H. B. van Linden van den Heuvell, *Phys. Rev. A* **46**, 2749 (1993).
 - [11] J. E. Bjorkholm and P. F. Liao, *Phys. Rev. Lett.* **33**, 128 (1974).
 - [12] D. S. Elliott, R. Roy, and S. J. Smith, *Phys. Rev. A* **26**, 12 (1982).
 - [13] M. M. Salour, *Ann. Phys. (N.Y.)* **111**, 364 (1978).
 - [14] J. Eberly and S. V. O'Neill, *Phys. Rev. A* **19**, 1161 (1979).
 - [15] G. N. Sinclair and M. W. Hamilton, *Rev. Sci. Instrum.* **65**, 2180 (1994).
 - [16] M. J. Ehrlich, L. C. Phillips, and J. W. Wagner, *Rev. Sci. Instrum.* **59**, 2390 (1988).
 - [17] P. T. Greenland, *J. Phys. B* **17**, 1919 (1984).
 - [18] E. Wolf, *Proc. R. Soc. London* **230**, 246 (1955).